Using Remotely Sensed Planetary Boundary Layer Variables as Estimates of Areally Averaged Heat Flux

R. L. Coulter, T. J. Martin, and D. J. Holdridge
Argonne National Laboratory
Argonne, Illinois

Introduction

Homogeneity across the Southern Great Plains (SGP) Cloud and Radiation Testbed (CART) site is an issue of importance to all facets of the Atmospheric Radiation Measurement (ARM) Program. The degree to which measurements at the central facility can be used to verify, improve, or develop relationships in radiative flux models that are subsequently used in global circulation models, for example, is tied directly to the representativeness of the local measurements at the central facility for the site as a whole.

The relative variation of surface energy budget terms over a 350-km x 400-km domain such as the SGP CART site can be (and is) extremely large. The Planetary Boundary Layer (PBL) develops as a result of energy inputs from widely varying surfaces. The lower atmosphere effectively integrates the local inputs; measurements of PBL structure can potentially be used for estimates of surface heat flux over scales on the order of tens of kilometers. This project is focusing on two PBL quantities that are intimately tied to the surface heat flux: 1) the height of the mixed layer, z_i, that grows during daytime due to sensible heat flux input from the surface; and 2) the convective velocity scale, w*, normally a scaling parameter defined by the product of the sensible heat flux and z_i, but in this case defined by coherent structures (thermal plumes in the convectively unstable PBL) that connect the surface layer and the capping inversion that defines z_i.

Variability of Heat Flux Across the CART Site

Figure 1 illustrates the variability of sensible heat flux, H, at 1230 local solar time (LST), across the SGP CART site over monthly periods, expressed in terms of the square root of the normalized spatial variance, V_s, and the normalized temporal variance, V_t:

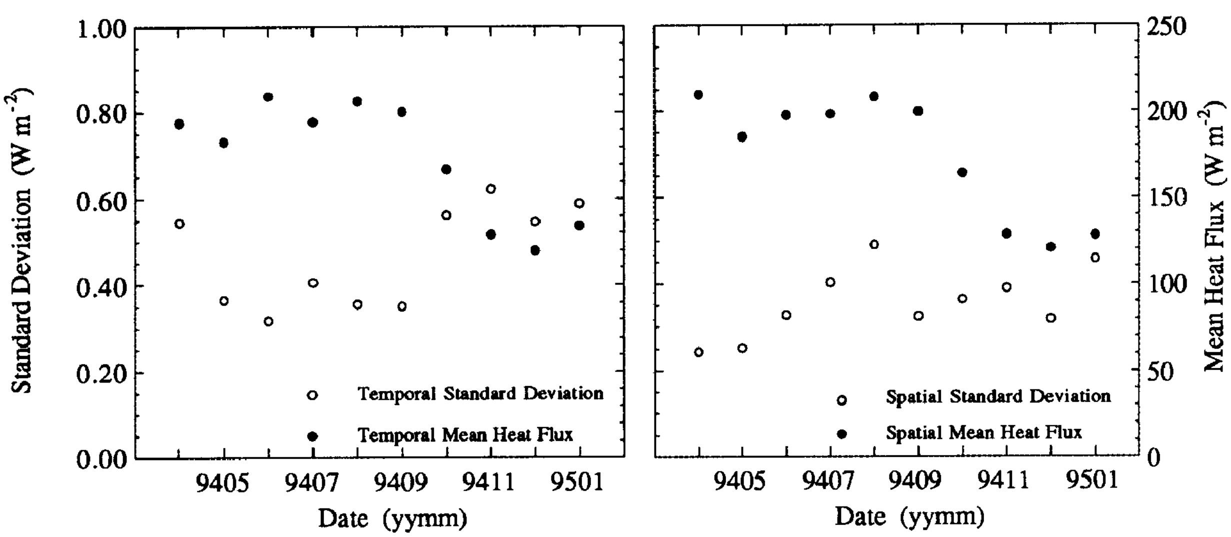

Figure 1. Temporal and spatial standard deviation of sensible heat flux over the SGP CART site. Values are normalized by the mean sensible heat flux, as defined in the text.

$$V_t = \frac{\sum_{i=1}^{N}\sum_{t=1}^{M}\left(H_{i,t} - \overline{H_t}\right)^2}{\sum_{i=1}^{N}\sum_{t=1}^{M} H_{i,t}^2} \qquad V_s = \frac{\sum_{t=1}^{N}\sum_{i=1}^{M}\left(H_{i,t} - \overline{H_s}\right)^2}{\sum_{t=1}^{M}\sum_{i=1}^{N} H_{i,t}^2} \tag{1}$$

$$\overline{H_t} = \frac{1}{M}\sum_{t=1}^{M} H_{i,t} \qquad \overline{H_s} = \frac{1}{N}\sum_{i=1}^{N} H_{i,t}$$

where $H_{i,t}$, is the sensible heat flux measured at site *i* and time *t* and where H_i and H_s are the temporal and spatial means, respectively. Values provided from the Energy Balance Bowen Ratio (EBBR) systems were modified with an aerodynamic calculation of H when the Bowen ratio $(\beta = H/LE)$ was between -0.75 and -1.25 (Wesely et al. 1995). Large values (>0.5) in Figure 1 are invariably associated with small mean values, usually during heavily overcast or precipitation conditions. The magnitude of the spatial variance is only slightly smaller than the temporal values. The true spatial variance may well be larger because present locations for heat flux measurements are solely over pasture and grassland. The partitioning of energy among ground, latent, and sensible fluxes will likely be different over cultivated fields such as wheat and alfalfa, which are currently being instrumented.

The primary causes of the spatial variability likely are local values of soil type, soil moisture, and cloud cover. Climatological variations such as NW-SE gradients in rainfall and cloudiness are compounded by local, short-term events such as recent rainfall, weather systems, and local circulations within the CART site. In addition, reductions in net radiation due to transient fair-weather cumulus clouds that dominate over the site can change local short-term (30-min) measurements of heat flux considerably.

Planetary Boundary Layer Estimates of H

Mixed Layer Height

The growth of the mixed layer during daytime is driven primarily by sensible heat flux to the atmosphere from the surface. Boers et al. (1984) developed relationships for the rate of rise of z_i. In the absence of entrainment,

$$\frac{dz_i}{dt} = \frac{H}{c_p \; z_i} \tag{2}$$

where γ is the lapse rate through the capping inversion, c_ρ is the density of air, and c_p is the heat capacity of air at constant pressure. With entrainment,

$$\frac{dz_i}{dt} = \frac{C_w}{\left(B + \frac{gz_i\delta\theta}{T_0\sigma_w^2} - \frac{A(\delta u)^2}{\sigma_w^2}\right)} \tag{3}$$

where C, B, and A are constants parameterizing entrainment of heat flux, $\delta\theta$ and δu are the temperature and horizontal wind speed jumps across the capping inversion, T_0 is the surface temperature, and σ_w is the standard deviation of vertical velocity. In convective conditions, B = A = 0, and Equation (3) becomes

$$\frac{dz_i}{dt} = \frac{CT_0\sigma_w^3}{gz_i\delta\theta} \rightarrow \frac{CH}{\rho c_p \delta\theta} \tag{4}$$

where σ_w^3 has been equated to the convective velocity scale (see below). We see that both Equations (2) and (4) relate the growth rate directly to the surface heat flux.

Because z_i usually reaches 1 to 3 km in convective conditions, one might expect that surface influences over a scale roughly 10 km or larger contribute to mixed layer growth when advective effects are included. An important point is that an instantaneous measurement of z_i is related to H_l, the time-integrated value of H since mixed layer growth began. This fact is useful because it provides a method for reducing the effects of short-time fluctuations on H (such as cumulus clouds suggested previously) when calculating spatial variability. Figure 2a shows an example of the variation of H, H_l, and z_i during daylight hours, and Figure 2b shows the relationship between z_i at the central facility and H_l over an extended period in July-August 1994. When H_l is averaged over sites neighboring the central facility, the correlation between z_i and H_l is considerably improved (Figure 2b). It is not immediately evident that including neighboring extended facilities should improve the correlation because those facilities are separated by roughly 50 km; the averaging process may account for some of the local variability near the central facility. Additional measurements in upcoming Intensive Operating Periods (IOPs) may be able to address this question directly.

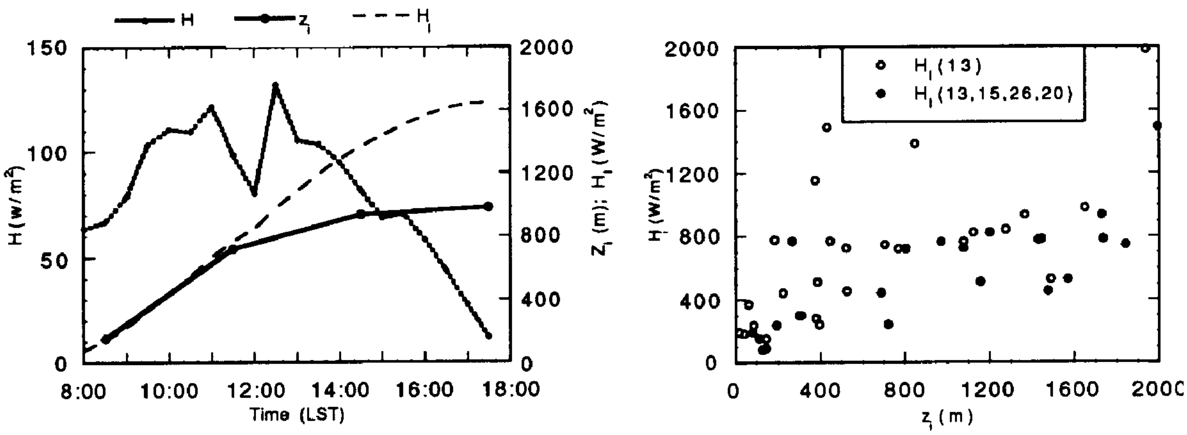

(a) (b)

Figure 2. (a) Variations of heat flux, integrated heat flux, and mixed layer depth at the central facility on July 23, 1994; (b) Variation of mixed layer height at central facility (site No. 13) with integrated heat flux at the central facility and integrated heat flux averaged for the central facility and neighboring extended facilities. The time step for integration is 30 min.

Coherent Structures

The primary method by which the PBL transfers energy from the surface through the mixed layer into the capping inversion is through coherent structures such as thermal plumes (Coulter et al. 1993; Stull 1989). Because these structures maintain their identity for 30-60 min and move with the mean wind, they effectively integrate over the surfaces over which they travel. The convective velocity scale, w*, is a measure of the strength of that transfer,

$$w^{*3} = \frac{g}{T_0}\frac{H}{\rho c_p} z_i \qquad (5)$$

where g is acceleration due to gravity. Some researchers (e.g., Boers et al. 1984) have chosen to define a measurement of w* in terms of the standard deviation, σ_w, of the vertical velocity, w. We choose to estimate w* by equating it with the vertical velocity associated with the thermal plumes most responsible for energy transfer because of their well-defined lifetime. In particular, we postulate that

$$w* = \alpha w_T(0.5z_i) \qquad (6)$$

where $w_T(0.5z_i)$ is the mean vertical velocity measured within thermal plumes at $z = z_i/2$ and α is a constant to be determined. We investigated this relationship with data from the Boardman ARM Region Flux Experiment (BARFEX) in 1992 (Doran et al. 1992). We used minisodar data within the lowest 200 m above desert steppe to select well-organized thermal plumes (defined as times with w > 15 cm/s for at least 25 s). The vertical velocity profile within the thermal plumes was then modeled as

$$w_T = a + b\sin(z\pi/z_i) \qquad (7)$$

and extrapolated (where necessary) to $z_i/2$ to provide an estimate of $w_T(0.5z_i)$. Airsonde launches provided measurements of z_i, and H was calculated from an average of three eddy correlation stations located in the steppe region. Figure 3 shows the relationship between $w_T(0.5z_i)$ and w* that suggests a value of $\alpha = 1.1$.

During an IOP in October 1994, the 915-MHz wind profiler was operated in a vertical-only mode that allowed estimates of w to be made every 15 s. Although this sample rate is roughly 10 times slower than that used with the minisodar, it was sufficient to sample coherent structures within the mixed layer in light wind conditions. The profiler provided direct estimates of w_T, as well as estimates of z_i, through inspection of the vertical time section of the intensity of the signal return and through analysis of Balloon Borne Sounding System (BBSS) launches from the central facility. Data were limited to 1200 to 1600 LST each day for two weeks. In this case, the thermal plumes were defined by using a wavelet transform technique described by Coulter and Li (1995). Values of $w_T(0.5z_i)$ within the regions selected were limited to those greater than 15 cm/s. The averaging time required by the profiler approximated the time for thermal definition used with the BARFEX data.

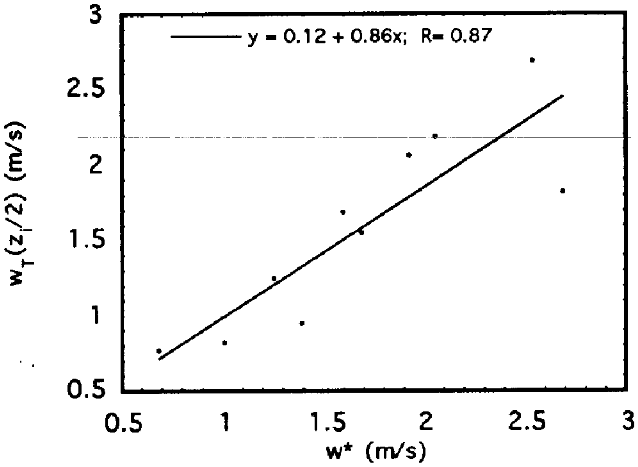

Figure 3. Modeled mid-thermal vertical velocities (from minisodar profiles) as a function of w* obtained above desert steppe on June 5 and June 14, 1992.

Figure 4 shows the relationship between w* and w_T at the CART site. In this case a value of α=1.1 again seems appropriate. The coefficient required may be greater than 1 because of incomplete sampling of the thermal plumes (sampling the edge rather than the center of the plume) or

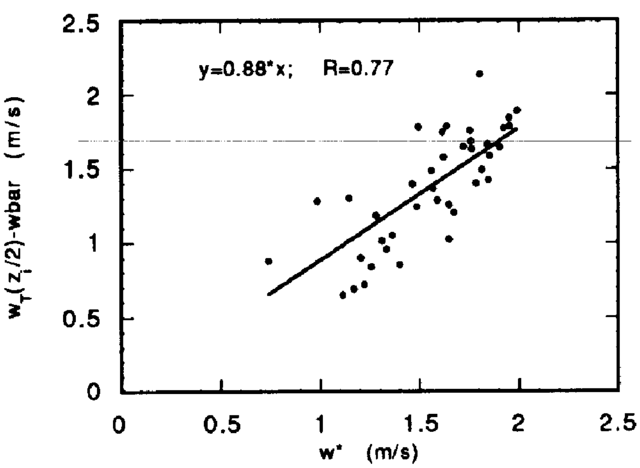

Figure 4. As in Figure 3, except mid-mixed layer vertical velocities are calculated directly from 915-MHz profiler data between Oct. 10 and Oct. 23, 1994 at the central facility of the SGP CART site.

because of non-representative estimates of H at the central facility. If so, these data would suggest that local H is larger at the central facility than at surrounding areas during the IOP. Future IOPs will focus on answering some of these questions and developing methods to use more rapid sampling of the vertical component of motion without compromising mean horizontal wind data.

References

Boers, R., E. W. Eloranta, and R. L. Coulter. 1984. Lidar observations of mixed layer dynamics: Tests of parameterized entrainment models of mixed layer growth rate, *J. Appl. Meteorol.*, **23**, 247-266.

Coulter, R. L., T. J. Martin, and D. R. Cook. 1993. Areally averaged estimates of surface heat flux from field studies for the Atmospheric Radiation Measurement program. In *Proceedings of the Third Atmospheric Radiation Measurement (ARM) Science Team Meeting, 1-4 March 1993*, Norman, Oklahoma, pp. 317-322. CONF-9303112, U.S. Department of Energy, Washington, D.C.

Coulter, R. L., and B. L. Li. 1995. A technique using the wavelet transform to identify and isolate coherent structures in the planetary boundary layer. In *Proceedings, 11th Symposium on Boundary Layers and Turbulence, 27-31 March 1995*, Charlotte, North Carolina.

Doran, J. C., F. J. Barnes, R. L. Coulter, T. L. Crawford, D. D. Baldocchi, D. R. Cook, D. Cooper, R. J. Dobosy, L. Fritschen, R. L. Hart, L. Hipps, J. M. Hubbe, W. Gao, R. R. Kirkham, K. E. Kunkel, T. J. Martin, T. J. Meyers, W. Porch, J. D. Shannon, W. J. Shaw, E. Swiatek, and C. D. Whiteman. 1992. The Boardman Regional Flux Experiment, *Bull. Amer. Meteorol. Soc.*, **73**, 1785-1795.

Stull, R. B. 1989. *An Introduction to Boundary Layer Meteorology*. Kluwer Academic Publishers. Boston, Massachusetts.

Wesely, M. L., D. R. Cook, and R. L. Coulter. 1995. Surface heat flux data from energy balance Bowen ratio systems. In *Proceedings, Ninth Symposium on Meteorological Observations and Instrumentation. 27-31 March 1995*, Charlotte, North Carolina.